Applied Science and Engineering Progress, Vol. 20, No. 3, 2027, 8289

Research Article

Properties of Argon Plasma Jets and Their Application to Enhance the Mycelium Growth of Lion's Mane (Yamabushitake) Mushroom

Wuttipong Ruksavong and Vilai Rungsardthong
Department of Agro-Industrial, Food, and Environmental Technology, Faculty of Applied Science, Food and Agro-Industrial Research Center, King Mongkut's University of Technology North Bangkok, Thailand

Lueacha Tabtimmai and Saranya Sedtananun
Department of Biotechnology, Faculty of Applied Science, Food and Agro-Industrial Research Center, King Mongkut's University of Technology North Bangkok, Bangkok 10800, Thailand

Salinee Acharry, Tanapol Kosolwattana, and Dusit Ngamrungroj*
Department of Social and Applied Science, College of Industrial Technology, King Mongkut's University of Technology North Bangkok, Bangkok 10800, Thailand

Rattachat Mongkolnavin
Department of Physics, Faculty of Science, Chulalongkorn University, Bangkok 10330, Thailand

Kewalee Nilgumhang
Thailand Institute of Nuclear Technology (Public Organization), Ongkharak, Nakhon Nayok 26120, Thailand

Prajya Tangjitsomboon
Faculty of Health Science and Technology, Navamindradhiraj University, Bangkok 10130, Thailand

Kanchaya Honglertkongsakul
Department of Physics, Faculty of Science, Burapha University, ChonBuri 20131, Thailand

* Corresponding author. E-mail: dusit.n@cit.kmutnb.ac.th DOI: 10.14416/j.asep.2026.09.003
Received: 16 February 2026; Revised: 17 March 2026; Accepted: 17 April 2026; Published online: 2 September 2026
© 2026 King Mongkut's University of Technology North Bangkok. All Rights Reserved.

Abstract
Lion's Mane (LM) mushroom requires around 32-35 days for its mycelium to reach full growth. The reduction of their mycelial growth would improve the cultivation efficiency and reduce the operation cost. This research aimed to study the properties of the argon plasma jet and its application in promoting the mycelial growth of LM mushrooms. A plasma jet was generated by varying the electrical frequency between 5 and 12 kHz and the argon gas flow rate of 5-8 L/min. Using a 9 kHz frequency with a gas flow rate of 7 L/min resulted in the maximum electrical power and the longest plasma beam length. An electron temperature range of 0.29-0.37 eV was observed when the electrical frequency was 6-12 kHz with the argon flow rate of 7 L/min. The mycelium growth of the LM mushroom was stimulated with different treatment times, 0-300 s. A morphological study by field emission scanning electron microscopy (FE-SEM) showed that plasma treatment could stimulate mycelium branching and formation, while treatments longer than 240 s resulted in severe burning and damage to the mycelium. During the cultivation period of 26 days, the plasma treatment at 30 s and 90 s indicated the highest average growth rate of mycelium at 0.41 cm/day, which was significantly faster than the control (0.18 cm/day). The mycelium growth enhancement could be due to the oxidative stress from reactive oxygen and nitrogen species (RONS), which stimulate the formation of sclerotia structures and increase the survival rate of the mushroom cells. The results obtained demonstrated that plasma jet technology is an effective option to accelerate the mycelial growth of the LM mushroom.

Keywords: Electron temperature, Lion's Mane mushroom, Mycelium, Plasma jet, Yamabushitake mushroom growth

1 Introduction

Plasma technology is gaining widespread attention for biological applications, especially for disinfection and sterilization, because of its microbial inhibition effects [1]. Atmospheric cold plasma generation becomes more and more popular due to its low operational cost and residue-free nature, and has been used in various fields such as extending the postharvest shelf life of strawberries [2] and controlling toxigenic fungi and mycotoxins in food [3]. The reaction of free radicals and charged particles in plasma can inhibit mould, bacteria, and viruses that cause plant diseases [1], [4], reduce the risk of fungal toxins (mycotoxins) [5], and stimulate seed germination [6] without the use of chemicals. Consequently, cold plasma using a plasma jet is a technology that is in line with the chemical-free concept, safe and sustainable agriculture. Cold plasma is also used in shelf-life extension of various mushrooms and to control microbial contamination during the mushroom cultivations [7].

In addition, cold plasma has been utilized to improve water quality for agricultural and food-processing applications. Ungwiwatkul *et al.,* [8] treated cold plasma on wastewater to generate plasma-activated water enriched with essential nutrients, including nitrate and ammonium ions, which subsequently can be used as fertilizers. Thana *et al.,* [9] used cold plasma-treated water for antimicrobial contamination during oyster meat processing. These studies demonstrate the potential of cold plasma technology for enhancing water quality and improving microbial safety in agricultural and food production systems.

Plasma jet, one of the most popularly used atmospheric cold plasma generators, produces a directed plume of ionized gas containing energetic electrons, ions, radicals, and excited species for applications in surface treatment, sterilization, material processing, and biomedical fields [10]. Flowing gas is an essential parameter to create the plasma jet. Common gases, including oxygen, nitrogen, helium, argon, or their mixtures [11], are used. The choice of gas affects the ions produced, and consequently, the reactions that occur. Furthermore, the energy used to generate the plasma jet affects the plasma properties, namely electron temperature and electron density [12], which in turn affect the mushroom mycelium being stimulated.

The biochemical mechanism of elicitation by cold plasma can be explained as follows. When argon gas is electrically excited to the point of becoming plasma, high-energy electrons and excited argon atoms (Argon metastable) are generated. As the excited argon atoms are ejected from the nozzle, they come into contact with or collide with the air surrounding the nozzle, which is filled with oxygen (O_2), nitrogen (N_2), and water vapor (H_2O). Energy from the argon plasma is transferred to molecules in the air, breaking the bonds of O_2, N_2, or H_2O in the surrounding air. These molecules then immediately reform into RONS (reactive oxygen and nitrogen species) before coming into contact with the surface of the target object [12],[13].

Lion's Mane (LM) or Yamabushitake mushroom is a medicinal mushroom that contains several bioactive compounds affecting the brain and nervous system by stimulating nerve growth factor (NGF) to improve concentration and memory. LM mushroom could prevent Alzheimer's disease in animal studies, reduce stress and depression, and also help strengthen immunity [14]. Many benefits of digestion aids, anti-inflammatory effects, high antioxidants, and fat burning by LM mushroom were reported [15], [16]. However, mushroom cultivation with careful environmental controls and growing conditions such as temperature and humidity is required to produce bioactive compounds from the mushroom. Generally, LM mycelium takes around 32-35 days for its full growth. Thus, the reduction of mushroom cultivation time would help farmers to increase cultivation cycles and reduce the operation cost [17].

Limited research on the use of plasma technology to stimulate mushroom growth has been reported. Agun *et al.,* [18] used plasma treatment to increase the germination rate and yield of mushrooms. Plasma stimulation enhanced the mycelial growth of the oyster mushroom (*Pleurotus ostreatus*) compared with the untreated one. Oon *et al.,* [19] used plasma to improve the mycelial growth of the gray oyster mushroom. Improvements in water absorption properties and the mushroom growth rate were obtained. Furthermore, Li *et al.,* [20] found that cold atmospheric plasma (CAP) can promote the growth of Lingzhi mushroom (*Ganoderma lucidum*) [20]. A 40-second plasma treatment once a week resulted in a 33.63% increase in average stem length and a 28% increase in the number of mushrooms with a cap area greater than the average.

However, despite the increased interest in cold plasma technology for agricultural and biological applications, the impact of argon plasma parameters on Lion's Mane mushroom cultivation remains insufficiently understood. In particular, data on the influence of plasma properties such as electron temperature, electrical frequency, argon gas flow rate, and contact time on mycelial growth and mushroom yield are limited. Unsuitable plasma conditions can lead to oxidative stress or growth inhibition, highlighting the need for optimized treatment parameters. Therefore, an argon jet plasma was set up in this experiment and some properties of the argon plasma, such as power, electron temperature and density, were measured. The objectives of this study were to apply the argon plasma jet to stimulate the mycelial growth of the LM mushroom with different treatment times. Then, the mycelium characteristics and mycelium growth rates of LM mushrooms were determined in order to select the optimal conditions, including the plasma treatment in this study.

2 Materials and Methods

2.1 *Experiment setup and measurements*

The plasma jet consisted of a plasma generator made from a borosilicate glass tube, with a tapered end of a 3 mm outer diameter and an inner diameter of 1.5 mm. In the tube, there was an anode electrode made of tungsten with a diameter of 1 mm, while the other terminal was located at the tapered end. There was a connecting joint between the ends of both electrodes. A gas flow meter was used to adjust the argon gas at 0-10 L/min. The argon plasma jet and measurement setup are shown in Figure 1. The potential difference that occurred at the plasma generator head led to the plasma jet at the tapered end of the head. The experiments were conducted at the frequencies of 5, 6, 7, 8, 9, 10, 11 and 12 kHz and the argon flow rates of 5, 6, 7 and 8 L/min.

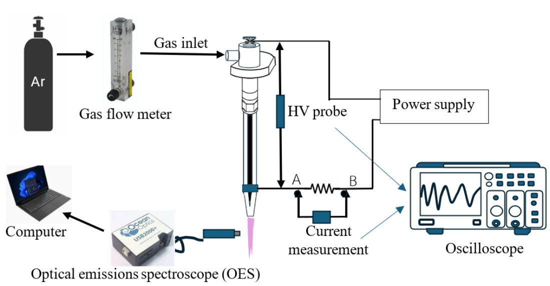

Figure 1: Plasma jet and measurement setup.

2.2 *Power measurement*

The power generated by the plasma was measured from the potential difference between the plasma source, which reduced the signal by 1000 times. The current was measured using potential difference (V_{AB}) across the resistor (R) 0.2 Ω, with a high voltage probe connecting to an oscilloscope (Tektronix TBS1022 25MHz 500 MS/s), in series with the circuit. The current was calculated based on Ohm's law ($I = \frac{V_{AB}}{R}$). The maximum power transmitted to the plasma was calculated from the following equation [12]:

$$P = I_m V_m \quad (1)$$

where P is the maximum power across argon plasma (W), I_m is the maximum current (A), and V_m is the maximum voltage (V).

2.3 *Electron temperature and electron density measurement*

Electron temperature (T_e) was determined by the Boltzmann plot and two intensity ratios [21], [22]. Partial local thermodynamic equilibrium (LTE) was assumed in the plasma generated due to the high frequency of particle collisions under air pressure. The spectra of argon plasma were determined using the Ocean Optic HR4000 spectrometer (200-1100 nm). Each peak from ArI and ArII spectra is selected based on the highest transition probability and then utilized to determine electron temperature by following the equation [21], [22]:

$$\frac{I_2}{I_1} = \frac{g_{i2}}{g_{i1}} \frac{A_{ij2}}{A_{ij1}} \frac{\lambda_1}{\lambda_2} \exp\left(-\frac{E_{i2} - E_{i1}}{k_B T_e}\right) \quad (2)$$

and the electron density (n_e) of argon plasma was also calculated using the following equation [23]:

$$n_e = 6.04 \times 10^{21} \frac{I_2}{I_1} \frac{g_{i2}}{g_{i1}} \frac{A_{ij2}}{A_{ij1}} \frac{\lambda_1}{\lambda_2} T_e^{\frac{3}{2}} \exp\left(-\frac{E_{j1} - E_{j2} + E_i}{k_B T_e}\right) \quad (3)$$

where I_1 and I_2 represent the intensity of the spectral line of ArI and ArII respectively, A_{ij1} and A_{ij2} are the transition probability of the transition from state to state j (the probability per second that an atom in upper-level state emits in a random direction, and is deexcited to a low-level state), g_{i1} and g_{i2} are the statistical weight of the upper level state, λ_1 and λ_2 are the wavelength of the line radiation, E_{j1} and E_{j2} are the energy of the upper level, k_B is the Boltzmann constant ($1.38x10^{-23}$ J/K), and T_e is the electron temperature. The values of wavelength (λ) and intensity (I) are obtained from the Optical Emission Spectroscopic, and the values of A_{ji}, g_i, and E_i are obtained from the National Institute of Standards and Technology (NIST) [24] atomic spectra database.

2.4 *Cultivation of LM mushroom*

The cultivation of LM mushrooms was carried out at Fresh & Friendly Farm Co., Ltd. (Pathum Thani, Thailand). LM inoculum was mixed with sterilized sorghum seed and incubated until full growth was obtained, which took around 7 days from the inoculation.

The mushroom medium (150 g), consisting of sawdust 70%, rice bran15%, and corncobs 15% by weight, was packed in 240 mL of autoclavable glass bottles and sterilized at 121°C for 30 minutes with a steam pressure of 1.5 bar (SX-700 Tomy, Japan). After cooling down the mushroom spawn to room temperature, the sorghum with inoculum 1% by weight prepared above was placed on the surface of the mushroom spawn before the plasma treatment.

2.5 *Treatment of LM mushroom spawn by argon plasma jet*

The mushroom spawns with inoculum on the top were treated with the argon plasma jet. The plasma jet with an input frequency of 9 kHz was selected since the maximum energy transfer, electron temperature and electron density were obtained at this condition (discussed in Sections 3.2 and 3.3). The distance between the end of the plasma jet tube and the mushroom culture was set at about 3 cm.

The plasma treatment durations were studied at 0 s, 30s, 60 s, 90 s, 120 s, 180s, 240 s, and 300 s. At least 10 glass bottles were used for each treatment. The stimulated areas are in the range of 1.86±0.25 cm^2 to evaluate the morphological effects of plasma stimulation on mycelium. Samples were examined using a field emission scanning electron microscope (FE-SEM; SU5000, Hitachi, Ibaraki, Japan). The samples were fixed onto aluminum stubs and sputter-coated with a thin gold–palladium layer to improve their surface conductivity before the FE-SEM observation. Micrographs were acquired under high vacuum using a secondary electron detector (SE(L)). FE-SEM analysis was performed at an accelerating voltage of 5.0 kV, a magnification of ×1.00 k, a working distance of 11.4 mm, and an emission current of 131 µA.

The control (without plasma treatment) and all treated mushroom spawns were further incubated in the cultivation room, with the temperature controlled at 16–18 °C and the humidity at around 85%. The mycelium growth was observed and recorded for its mycelium length daily until 26 days, while the maximum height of the bottle was 8 cm. The experiments were carried out with at least three replications. The data were presented as the average and standard deviation.

3 Results and Discussions

3.1 *Properties of argon plasma jet*

3.1.1 Power measurement and plasma jet length

In this study, alternating current with different frequencies ranging from 5 to 12 kHz and the argon gas flow rate of 5 to 8 L/min were used to generate argon plasma discharge. The resulting voltage and current waveforms of the plasma jet from all configurations have a sine-like shape, which indicates a stable periodic discharge without intense current spikes, as shown in the example in Figure 2. The results obtained suggest that non-thermal plasma provides a more stable discharge than the arc-like discharge, which utilizes argon-based gas mixtures or operates under higher-power conditions [10]. Additionally, these configurations provide uniform energy distribution during plasma production, which differs from previous studies on plasma jets that are characterized by severe current surges [25].

For argon plasma jet discharge, the Lissajous figures plot of voltage and current at different input frequencies and flow rates is shown in Figure 3. The data in Figure 3 show that at a gas flow rate of 7 L/min, the current and voltage increase within 5-9 kHz and decrease when the frequency increases to 9-12 kHz, while the maximum current and voltage are observed at 9 kHz. A similar trend was observed with all other argon flow rates tested.

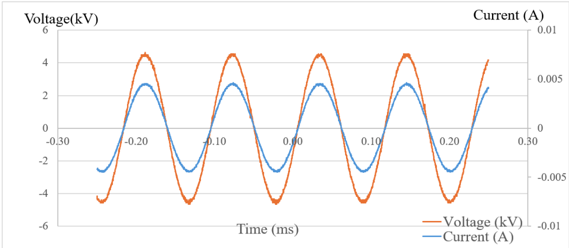

Figure 2: Voltage and current waveforms with input frequency at 9 kHz and argon flow rate of 7 L/min.

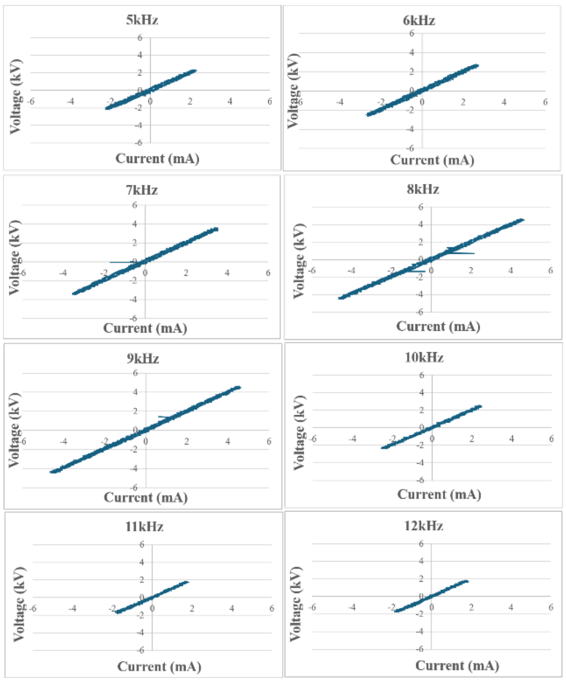

Figure 3: Lissajous curves with different input frequencies and argon gas flow rate at 7 L/min.

The powers in the plasma region, calculated from I_m and V_m (equation 1) with different frequencies and argon flow rates, are shown in Figure 4. An increase in power is observed for the frequency 5 - 9 kHz; conversely, a decrease in power was revealed when the frequency increases from 9 - 12 kHz. The highest power was obtained at 9 kHz and the gas flow rate of 7 L/min. The results demonstrate clearly that for AC power, the frequency significantly affects the power transferred to the plasma. The power affects argon ionization, which further leads to the length of the argon plasma beam.

As shown in Figure 5, the lengths of the argon plasma beam vary between 0 and 2.2 cm depending on the frequency and the gas flow rate. The plasma jet length increased with an increase of frequency from 5 to 9 kHz, while a decrease in the plasma length could be observed with the frequencies from 10 to 12 kHz. This result aligns with the length of the argon plasma jet studied by Jarunsak [26], which reported the plasma length of 1 – 3 cm. The electrical power and length of the argon plasma jet at 9 kHz with an argon flow rate of 7 L/min led to the near circuit resonance condition in which most of the energy is transferred to the plasma.

3.1.2 Electron temperature and electron density

Considering the electric power energy transfer in Figure 4 (Section 3.1.1) and plasma jet length, the highest power energy transfer was revealed when an electrical frequency of 9 kHz and an argon gas flow rate of 7 L/min were applied. Therefore, the gas flow rate of 7 L/min with different electrical frequencies was selected for further study on the electron temperature and electron density of the plasma system. The spectrum emitted from the argon plasma jet for the wavelength 200 - 1100 nm, 9 kHz, and gas flow rate of 7 L/min, shown in Figure 6, can be separated into two groups. The first group with wavelengths 300 - 400 nm (UV-VB) indicates the spectra of nitrogen species [22], [27], while the second group with wavelengths 600-1000 nm is emitted from argon gas, which is in the visible light and NIR range. Several reports show similar results for the spectrum of the argon plasma jet, such as the study on the characteristics of an argon plasma jet generated by 50 Hz alternating current [12].

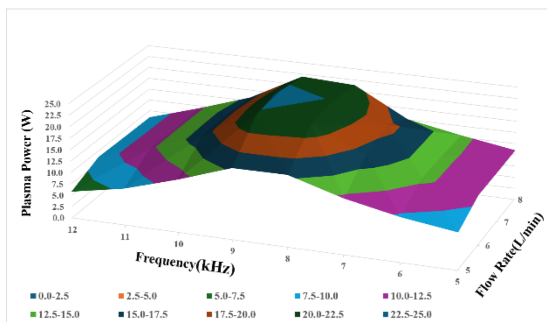

Figure 4: Electric power with different input frequencies and argon gas flow rates.

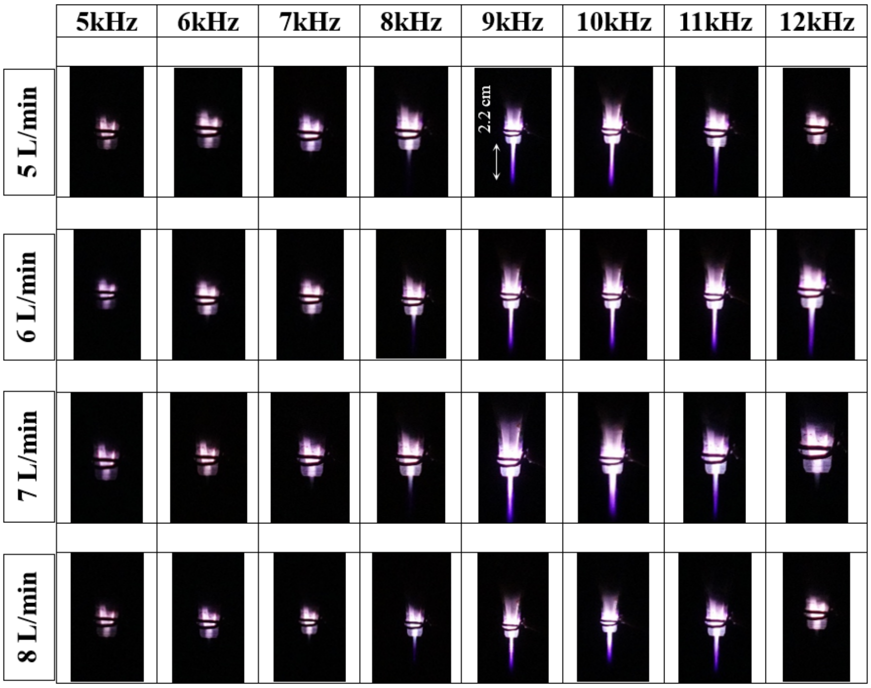

Figure 5: Length of argon plasma jet with gas flow rates at 5 - 8 L/min and input frequencies of 5 - 12 kHz.

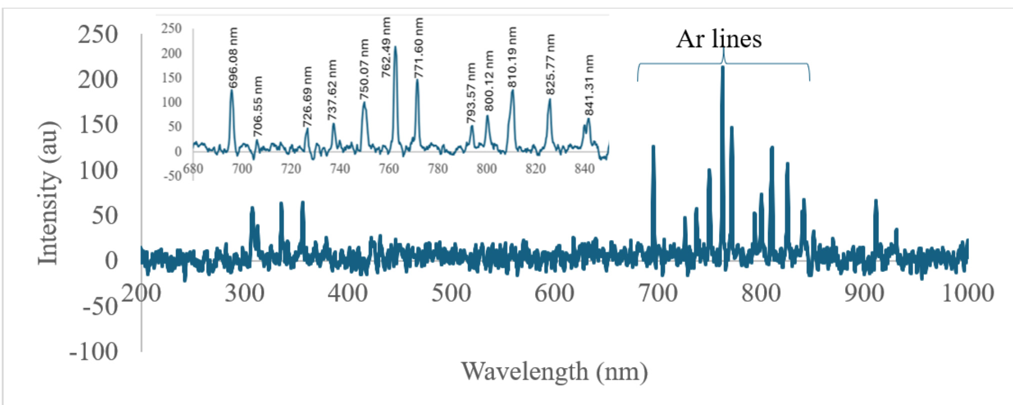

Figure 6: Argon spectrum of plasma with input frequency at 9 kHz and gas flow rate of 7 L/min.

Electron temperatures of the argon plasma jet exhibited in Figure 7 range from 0.29 to 0.37 eV, while their electron densities shown in Figure 8 are between 1.41×10^{10} to 8.59×10^{13} cm^{-3}. It can be seen that the increase in electron temperature (T_e) will increase the electron density, which corresponds with previous studies [12], [21]. However, compared to the study with 50 kHz and 5 - 12 kHz, the electron temperature was higher while the electron density was lower than the values obtained in our study.

When electrical power is coupled efficiently into the plasma discharge, the ionization of argon atoms is significantly enhanced, resulting in the rapid generation of free electrons through electron-impact ionization:

$$Ar + e^- \rightarrow Ar^+ + 2e^-$$

$$2Ar + 2e^- \rightarrow 2Ar^+ + 4e^-$$

Consequently, although the electron temperature (T_e) increases only slightly, the number of generated electrons can increase substantially, leading to a pronounced increase in the electron density (n_e).

The higher power output enhances energy transfer to the argon gas, resulting in more efficient plasma generation. Consequently, the plasma exhibits higher electron temperature and electron density, which indicate an increased concentration of energetic electrons within the plasma system. The presence of more energetic electrons promotes the formation of argon ions through electron-impact ionization. These argon ions subsequently interact with surrounding air molecules and moisture, leading to the generation of higher levels of reactive oxygen and nitrogen species (RONS).

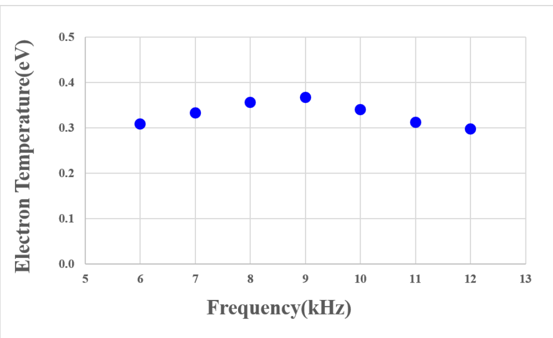

Figure 7: Electron temperature of argon plasma jet with the gas flow rate at 7 L/min.

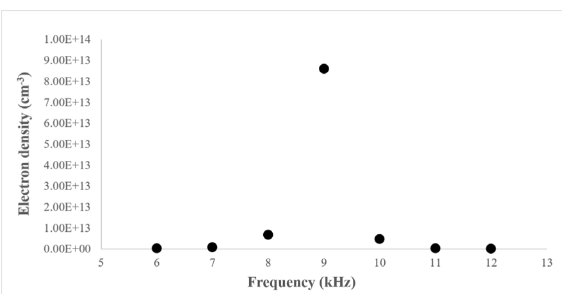

Figure 8: Electron density of argon plasma jet with the gas flow rate of 7 L/min.

During ionization, electrons provide the activation energy to overcome the molecular bonds, pushing molecules into highly excited, unstable, or dissociated states such as reactive oxygen and nitrogen. The energy described as electron temperature leads to ionized gas molecules through high-velocity collisions. Additionally, electrons can form negative ions through dissociative attachment, which later interact with the other air molecules to form heavier species. When the ionization rate surpasses the rates of attachment and recombination, the electron density (n_e) increases exponentially. Negative ion production is governed by electron density [28], [29]. Hence, the argon plasma jet with a frequency of 9 kHz and a gas flow rate of 7 L/min was selected for the stimulation of LM mushroom-mycelium growth. These conditions could maximize both T_e and n_e, assuming the most effective stimulation for mycelium extension.

3.2 *Effect of argon plasma jet on the LM mycelium growth*

Some areas of the plasma-treated mushroom surface are illustrated in Figure 9(a). Burn marks on the treated surface were observed after the treatment, as shown in Figure 9(b). Prolonged plasma exposure increased both the size and depth of the damaged areas, leading to the formation of larger and deeper holes.

Figure 10 exhibits the FE-SEM image (x1000) of the plasma-treated mushroom and the fully grown mycelium on the inoculated sorghum. It was found that the nontreated mycelium (control) was relatively straight with a diameter around 1.90 - 3.54 µm.

(a) (b)

Figure 9: Plasma treatment on LM mushroom inoculum using argon plasma jet (a), appearance of the inoculum after treating with the argon plasma jet (b).

Applied Science and Engineering Progress, Vol. 20, No. 3, 2027, 8289

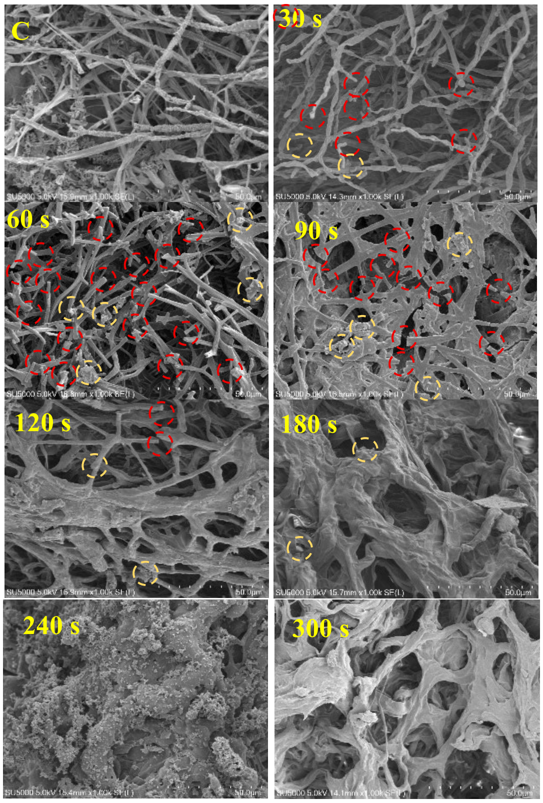

Figure 10: FE-SEM images of mycelium of Lion's Mane Mushroom after treatment with argon plasma jet at 9 kHz, flow rate 7 L/min, and magnification ×1,000.

After 30 s of treatment, the mushroom mycelium exhibited some physical changes compared to the control, including smaller mycelium sizes (0.6 - 2.42 µm) and some restricted areas shown. With 60 s of plasma stimulation. The mushroom mycelia were shrunk, which might be due to moisture loss. Some mycelium cut/damages (red circle in Figure 10) are observed, separating them into shorter mycelium, which then fuse or connect with other mycelium, forming branching structures. The mycelium diameters of the 60 s treatment are approximately 1.14 - 2.98 µm. Upon plasma treatment at 90 s, approximately the same diameter (1.12 - 2.64 µm) of the 60 s treatment, however rather flat with rougher and drier surface of the mycelia were observed. It is assumed that moisture was almost removed, and increasing branching of the mycelia occurred. After the plasma treatments for 120 s and 180 s, the mycelia fused together into a sheet with a fused area of approximately 14.5 - 18.6 µm. The broken mycelia were still present (red circle in Figure 10), albeit in reduced quantity, and sclerotia structures (yellow circle in Figure 10) were also observed.

After 240s for the treatment, the mycelium fused and burned, resulting in a splintered appearance. Excessive damage to the mushroom mycelia was discovered covering all over the entire mycelium surface with 300 s treatment, splintered, burnt parts detached, revealing a large, fused mass of mycelium. In conclusion, the mushroom mycelium indicated an inferior quality of the mycelium formed with the excessive plasma treatment at 240s and 300s.

Argon plasma jet treatment or stimulation significantly influenced the surface morphology, chemical functional groups, and surface hydrophilicity of fungal mycelia through the action of reactive oxygen and nitrogen species (RONS) generated during plasma discharge [19]. Prolonged plasma treatment led to increased surface indentations, cracks, and structural fractures in the fungal hyphae. These morphological changes may be associated with the formation of sclerotial structures (yellow circle in Figure 10) and partial degradation of the cell wall [19], [30]. Oxidative stress induced by RONS promoted sclerotia formation as a protective survival response. As the plasma exposure time increased, the mycelium structure became progressively more folded, deformed, and collapsed due to oxidative damage and plasma-induced reactions occurring on the mushroom surface [19]. However, the RONS and intracellular oxidative stress markers were not directly measured in this study. Future studies on the effects of prolonged plasma exposure on oxidative stress and sclerotia formation are required to fully understand their relationship.

Prolonged exposure to plasma results in significant growth inhibition of the fungus [25]. Initial treatment durations are sufficient to disrupt the fungal hyphae structure; however, extended exposure further degrades both the hyphae and the internal structures of the sclerotia. Consequently, the experiments conducted between the 30s and 90s showed that the hyphal structure was not destroyed but rather fragmented. When the stimulation time was increased to 120s and 180s, the fungal hyphae began to undergo structural destruction. Conversely, exposure times of 240s and 300s were considered excessive, destroying both the hyphae and the sclerotial tissues, as clearly seen by the FE-SEM image, leading to lower mycelium growth compared to 30 - 90s plasma treatment, as explained in the next experiment. Thus, this study focuses on treating time from 30 180s.

3.3 *Effect of plasma treatments on mycelial growth of LM mushroom*

Generally, for LM mushroom cultivation, the mycelium growth rate correlates well with the growth rate and weight of the fruiting bodies formed in further incubation. Thus, the mycelium growth rate in each condition was determined and compared in this study. Daily growth of the LM mushroom mycelium of the control and plasma-treated samples during 26 days of incubation in the glass bottles is presented in Figure 11. The mycelium growth stage could be divided into four stages as follows: The first lag stage (I) for the first three days, the mycelium adaptation or acclimation period of the mycelium for the new environment and accumulating nutrients before entering the exponential growth phases in the second stage (II), 3 - 11 days, and the third stage of the incubation. During the third stage, sclerotia structures developed rapidly, resulting in faster growth than in the other phases [18].

The third stage (III), during 11 - 20 days, the treated with all conditions started to grow more rapidly than the control, while different treatment times showed different results. The fourth stage (IV), from day 20, the growth of treated LM mushrooms began to enter the stationary phase, while 30 - 90s treatment reached the maximum height of the cultivation bottle at 8 cm.

Additionally, the mycelium growth response could be classified as the control, the short-exposure group (30s, 60s, and 90s), and the long-exposure group (120s and 180s). The control group showed an average mycelium growth rate of 0.179±0.059 cm/day. During the early cultivation period from day 3 to day 4, the plasma-treated mushrooms exhibited a relatively high mycelium growth rate, while the growth rate became close to that of the control during days 5 - 12. A clear difference among the treatment groups was observed from day 12 - 20, where the short-exposure group (30s, 60s, and 90s) showed a mycelium growth rate of 0.607±0.017 cm/day, while the longer exposure group (120s and 180s) showed a lower rate of 0.393±0.033 cm/day. After day 20, the growth rate decreased in both plasma-treated groups, with 0.170±0.020 cm/day for the short-exposure group and 0.083±0.006 cm/day for the long-exposure group. Considering the whole cultivation period from day 3 - 26, the short-exposure group showed the highest average mycelium growth rate of 0.413±0.052 cm/day, followed by the long-exposure group at 0.284±0.015 cm/day, compared to 0.179±0.059 cm/day of the control. These results indicate that short argon plasma jet exposure promoted mycelium growth more effectively than longer exposure durations.

Figure 12 shows the mycelium growth of LM mushrooms for 26 days of cultivation. The mycelium in the 30s, 60s, and 90s treatments exhibited denser and more uniform mycelium colonization than the control. In contrast, the 120s and 180s treated samples showed less uniform mycelium development, and non-utilized substrates were visually observed. This observation supports

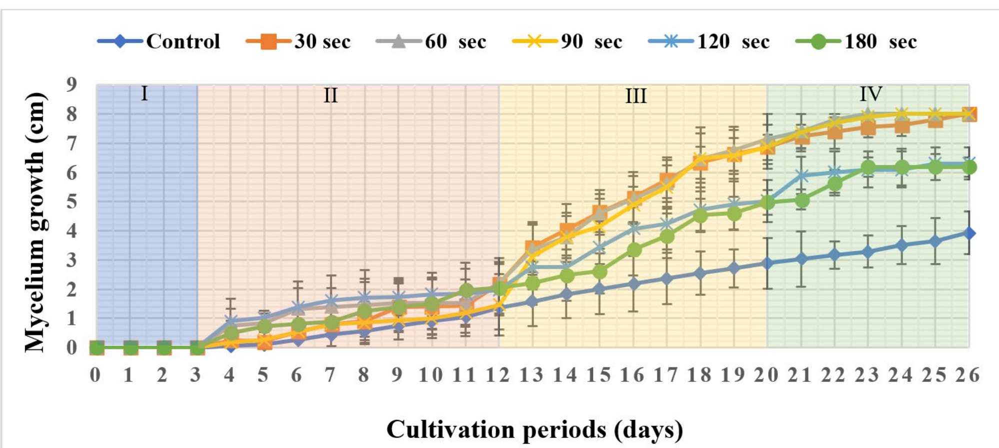

Figure 11: Mycelium growth of LM mushroom with different plasma treatment times, at 9 kHz and a gas flow rate of 7 L/min. Control is the cultivation without plasma treatment.

Figure 12: Mycelial growth of Lion's Mane mushroom in the control and plasma-treated at different times.

the finding that plasma treatment or exposure time significantly affected mycelium growth, whereas longer exposure may damage the mycelium as described above by FE-SEM images and reduce the stimulatory effect of the argon plasma jet.

Hyphal fragmentation, mitotic spore formation, and sclerotia development are important mechanisms of asexual fungal reproduction. Plasma-generated reactive oxygen and nitrogen species (RONS) may stimulate hyphal fragmentation and cellular activity, promoting rapid mycelium expansion and colony formation. Since asexual reproduction requires less energy and occurs faster than sexual reproduction, plasma stimulation may enhance fungal growth efficiency and adaptation [1], [31].

The main advantage of argon plasma jet stimulation is its ability to promote mycelium growth within a short treatment period, especially at 30 – 90s, where denser and more uniform colonization was observed. This suggests that a suitable plasma dose may activate fungal surface responses, enhance hyphal fragmentation, and support rapid mycelium expansion. However, excessive plasma exposure is a major limitation because longer treatments of 120s and 180s produced visible surface damage, lower growth uniformity, and reduced growth rate. These effects may be related to excessive dehydration, thermal accumulation, and oxidative stress caused by prolonged interaction with plasma-generated reactive species [32]. Therefore, plasma treatment should be carefully performed by controlling exposure time, plasma-to-sample distance, gas flow rate, and operating input frequency.

4 Conclusions

This research demonstrated the successful application of cold plasma jet technology using argon gas to stimulate and promote the mycelial growth of Lion's Mane mushroom. The electron temperature of the plasma obtained ranged from 0.29 to 0.37 eV. The maximum energy transfer of the argon plasma jet occurred at an electrical frequency of 9 kHz and a gas flow rate of 7 L/min, delivering 25.5 W of power, which is considered a safe and suitable cold plasma state for biological stimulation.

FE-SEM revealed that the duration of plasma contact with the mushroom mycelium significantly affects its physical structure. With 60s treatment, the contractile portions of the mycelium began to break down into smaller filaments and connect to form a branched structure. This phenomenon can be explained by stress from reactive species generated in the plasma. The optimum level of stress stimulates the mushroom cells to form sclerotia and accelerate growth to increase their chances of survival.

The growth rate of the mushroom mycelium during the 26-day cultivation period of the plasma-treated samples revealed a significant increase during growth stage 3 (days 11 – 20). Plasma stimulation for 30s and 90s resulted in the highest growth rate of 0.413±0.052 cm/day, compared with 0.179±0.059 cm/day in the control group. Treatment of the LM mushroom inoculum using the argon plasma jet successfully reduced the incubation period required for fully developed mycelium from 35 days in the control to only 26 days, representing a 25% improvement. The results may vary depending on the mushroom strain or environmental conditions. Future studies involving surface temperature monitoring, reactive species quantification, and biological viability assessment could further improve treatment uniformity and minimize plasma-induced damage while maintaining the growth-promoting effects.

Acknowledgments

This research was funded by the College of Industrial Technology, King Mongkut's University of Technology North Bangkok (Grant No. Res-CIT361/2024), program [grant number N23G660046] under the National Research Council of Thailand (NRCT) and Fresh and Friendly Farm Co., Ltd. for their financial supports.

Author Contributions

W.R.: investigation, methodology, writing an original draft and data equipment set up; V.R.: conceptualization, methodology, reviewing and editing, funding acquisition, project administration; L.T.: methodology, supervision; S.S.: supervision; S.A.: supervision; T.K: data analysis; D.N.: conceptualization, investigation, data analysis, data equipment set up, investigation, writing an original draft, reviewing and editing, funding acquisition; R.M.: conceptualization, methodology, supervision; K.N.: data analysis; P.T.: data analysis; K.H.: data analysis.

Conflicts of Interest

The authors declare no conflict of interest.

Declaration of generative AI and AI-assisted technologies in the writing process

The authors utilized the Gemini tool to enhance the language and readability of the manuscript.

References

[1] A. Sakudo, Y. Yagyu, and T. Onodera, "Disinfection and sterilization using plasma technology: Fundamentals and future perspectives for biological applications," *International Journal of Molecular Sciences*, vol. 20, no. 20, Art. no. 5216, Oct. 2019, doi: 10.3390/ijms20205216.

[2] N. N. Misra et al., "Cold plasma in modified atmospheres for post-harvest treatment of strawberries," *Food and Bioprocess Technology*, vol. 7, no. 11, pp. 3045–3054, Nov. 2014, doi: 10.1007/s19 47-014-1356-0.

[3] N. H. Neuenfeldt, L. P. Silva, R. S. Pessoa, and L. O. Rocha, "Cold plasma technology for controlling toxigenic fungi and mycotoxins in food," *Current Opinion in Food Science*, vol. 52, Art. no. 101045, Aug. 2023, doi: 10.1016/j.cofs.2023.101045.

[4] B. Adhikari, K. Pangomm, M. Veerana, S. Mitra, and G. Park, "Plant disease control by non-thermal atmospheric-pressure plasma," *Frontiers in Plant Science*, vol. 11, Art. no. 77, Feb. 2020, doi: 10.3389/fpls.2020.00077.

[5] B. Murtaza et al., "Cold plasma: A success road to mycotoxins mitigation and food value addition," *Food Chemistry*, vol. 445, Art. no. 138378, Jul. 2024, doi: 10.1016/j.foodchem.2024.138378.

[6] J. Orlowski et al., "Application of cold atmospheric pressure plasma jet results in achievement of universal antibacterial properties on various plant seeds," *Applied Sciences*, vol. 15, no. 3, Art. no. 1255, Jan. 2025, doi: 10.3390/app15031255.

[7] N. P. Minh, "Corona discharge power of plasma treatment influence on the physicochemical and microbial quality of enoki mushroom (*Flammulina velutipes*)," *Journal of Pure and Applied Microbiology*, vol. 16, no. 1, pp. 182–192, Mar. 2022, Art. no. 7258, doi: 10.22207/JPAM. 16.1.08.

[8] S. Ungwiwatkul, M. Jaikua, K. Prasertboonyai, P. Thana, A. Tamman, and K. Matra, "Plasma-activated municipal wastewater (PAMW): Revolutionizing municipal wastewater into high-value liquid fertilizer for duckweed cultivation through air plasma treatment," *Applied Science and Engineering Progress*, vol. 18, no. 3, Art. no. 7791, Jul. 2025, doi: 10.14416/j.asep.2025.04.002.

[9] P. Thana et al., "Development and application of a novel flow-through plasma-activated water generator for household food safety: Characterization, safety, and antimicrobial efficacy," *Applied Science and Engineering Progress*, vol. 19, no. 1, Art. no. 7901, Jan. 2026, doi: 10.14416/j.asep.2025.09.003.

[10] P. Buppan, N. Saengchan, K. Thongma, P. Phuangphuang, W. Sangwang, and K. Matra, "The efficiency of non-thermal plasma on the inhibition of environmental isolates of *Cryptococcus neoformans* from pigeon droppings," *Tropical Biomedicine*, vol. 42, no. 3, pp. 258–266, Sep. 2025, doi: 10.47665/tb.42.3.004.

[11] F. do Nascimento, S. A. Moshkalev, and M. Machida, "Changes in properties of dielectric barrier discharge plasma jets for different gases and for insulating and conducting transfer plates," *Brazilian Journal of Physics*, vol. 47, no. 3, pp. 278–287, Jun. 2017, doi: 10.1007/s13538-017-0492-1.

[12] K. Honglertkongsakul, K. Nilgumhang, R. Mongkolnavin, P. Tangjitsomboon, S. Acharry, and D. Ngamrungroj, "Characteristics of Ar plasma jet generated by 50 Hz alternating current," *Journal of Physics: Conference Series*, vol. 2013, no. 1, Art. no. 012005, Nov. 2021, doi: 10.1088/1742-6596/2013/1/012005.

[13] W. Seelarat et al., "Enhanced fruiting body production and bioactive phytochemicals from white *Cordyceps militaris* by blending *Cordyceps militaris* and using cold plasma jet," *Plasma Chemistry and Plasma Processing*, vol. 43, no. 1, pp. 139–162, Jan. 2023, doi: 10.1007/s11090-022-10292-w.

[14] Y. Y. Hwang, S. Sudirman, E. Wei, R. Shiu, Z. Kong, and D. Hwang, "Yamabushitake mushroom (*Hericium erinaceus* (Bull.) Pers. 1797) mycelium improves reproductive system dysfunction in male rats induced by polystyrene microplastics," *International Journal of Molecular Sciences*, vol. 26, no. 12, Art. no. 5735, Jun. 2025, doi: 10.3390/ijms26125735.

[15] S. P. Kim, M. Y. Kang, Y. H. Choi, J. H. Kim, S. H. Nam, and M. Friedman, "Mechanism of *Hericium erinaceus* (Yamabushitake) mushroom-induced apoptosis of U937 human monocytic leukemia cells," *Food & Function*, vol. 2, no. 6, pp. 348–356, Jun. 2011, doi: 10.1039/c1fo10030k.

[16] K. Hiwatashi et al., "Yamabushitake mushroom (*Hericium erinaceus*) improved lipid metabolism in mice fed a high-fat diet," *Bioscience, Biotechnology, and Biochemistry*, vol. 74, no. 7, pp. 1447–1451, Jul. 2010, doi: 10.1271/bbb.100130.

[17] P. Chutimanukul, W. Phatthanamas, O. Thepsilvisut, T. Chantarachot, A. Thongtip, and P. Chutimanukul, "Commercial scale production of Yamabushitake mushroom (*Hericium erinaceus* (Bull.) Pers. 1797) using rubber and bamboo sawdust substrates in tropical regions," *Scientific Reports*, vol. 13, no. 1, Art. no. 14210, Aug. 2023, doi: 10.1038/s41598-023-4061-y.

[18] L. Agun, A. H. A. A. Bakar, S. N. A. M. Azlan, N. A. S. C. M. Sukri, M. S. M. Deni, and F. A. A. Majid, "Spawn treatment by cold plasma to increase mushroom germination and production," *IOP Conference Series: Materials Science and Engineering*, vol. 884, no. 1, Art. no. 012004, Aug. 2020, doi: 10.1088/1757-899x/884/1/012004.

[19] F. M. Oon, L. Agun, M. F. I. Misnal, M. N. F. Zainal, N. Redzuan, and N. B. Ahmad, "Effect of cold plasma voltage and treatment duration on the microstructure and hydrophilicity of mushroom grain spawn," *Evergreen*, vol. 11, no. 1, pp. 379–385, Mar. 2024, doi: 10.5109/7172300.

[20] M. Li, X. Huang, and Z. Xiong, "Investigation of stimulated growth effect using pulsed cold atmospheric plasma treatment on *Ganoderma lucidum*," *Plasma Science and Technology*, vol. 24, no. 11, Art. no. 115503, Aug. 2022, doi: 10.1088/2058-6272/ac78cd.

[21] H. H. Kadhim, R. S. Mohammed, and M. A. Marjine, "Optical emission spectroscopy technique to estimation of electron temperature and density of plasma jet induced by applied AC high voltage," *Journal of Optics*, Mar. 2025, doi:10.1007/s12596-025-0267-x.

[22] S. H. Maan, "Construction of cold atmospheric pressure plasma jet system for treatment of germination and growth of iraqi wheat," M.S. thesis, Department of Physics, College of Science, University of Kerbala, Kerbala, Iraq, 2022.

[23] H. B. Baniya, R. Shrestha, R. P. Guragain, M. B. Kshetri, B. P. Pandey, and D. P. Subedi, "Generation and characterization of an atmospheric-pressure plasma jet (APPJ) and its application in the surface modification of polyethylene terephthalate," *International Journal of Polymer Science*, vol. 2020, Art. no. 9247642, Feb. 2020, doi: 10.1155/2020/9247642.

[24] E. B. Saloman, A. Kramida, Yu. Ralchenko, J. Reader, and NIST ASD Team, "NIST Atomic Spectra Database," National Institute of Standards and Technology, Gaithersburg, MD, USA, Tech. Rep. NIST ASD, Mar. 2019. [Online.] Available: https://www.nist.gov/pml/atomic-spectra-database

[25] S. Supakitthanakorn, O. U. Ruangwong, C. Sawangrat, W. Srisuwan, and D. Boonyawan,

"Potential of nonthermal atmospheric-pressure dielectric barrier discharge plasma for inhibition of *Athelia rolfsii* causing southern blight disease in lettuce," *Agriculture*, vol. 13, no. 1, Art. no. 167, Jan. 2023, doi: 10.3390/agriculture13010167.

[26] N. Jarunsak, "Development of an atmospheric pressure cold plasma jet for blood coagulation," M.S. thesis, Department of Biomedical Engineering, Faculty of Engineering, Bangkok, Thailand, 2017, doi: 10.58837/CHULA.THE.2017.1381.

[27] P. Thana et al., "Influence of pin-to-plane discharge modes on the physicochemical properties of single-pass flow-through plasma-activated water and its efficacy in agricultural applications," *IEEE Access*, vol. 14, pp. 192–207, 2026, doi: 10.1109/ACCESS.2025.3639415.

[28] K. McKay, J. S. Oh, J. L. Walsh, and J. W. Bradley, "Mass spectrometric diagnosis of an atmospheric pressure helium microplasma jet," *Journal of Physics D: Applied Physics*, vol. 46, no. 46, Art. no. 464018, Oct. 2013, doi: 10.1088/0022-3727/46/46/464018.

[29] S. K. Kc, B. Ghimire, S. H. Hong, J. S. Oh, and E. J. Szili, "How to control the plasma jet production of reactive species for medical therapy? A topical review," *Journal of Physics D: Applied Physics*, vol. 58, no. 14, Art. no. 143001, Mar. 2025, doi: 10.1088/1361-6463/adb316.

[30] T. R. Jørgensen et al., "Identification of SclB, a Zn(II)2Cys6 transcription factor involved in sclerotium formation in *Aspergillus niger*," *Fungal Genetics and Biology*, vol. 139, Art. no. 103377, Jun. 2020, doi: 10.1016/j.fgb.2020.103377.

[31] V. Scholtz, J. Pazlarova, H. Souskova, J. Khun, and J. Julak, "Nonthermal plasma-A tool for decontamination and disinfection," *Biotechnology Advances*, vol. 33, no. 6, pp. 1108–1119, Nov. 2015, doi: 10.1016/j.biotechadv. 2015.01.002.

[32] P. Bourke, D. Ziuzina, L. Han, P. J. Cullen, and B. F. Gilmore, "Microbiological interactions with cold plasma," *Journal of Applied Microbiology*, vol. 123, no. 2, pp. 308-324, Aug. 2017, doi: 10.1111/jam.13429.